
Multibeam Effects on Fast-Electron Generation from Two-Plasmon-Decay Instability

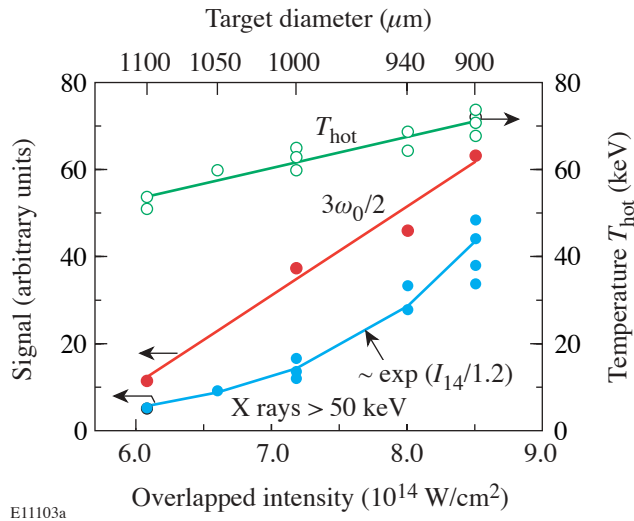
Two-plasmon-decay (TPD) instability has long been identified as a potential source for suprathermal electrons that can pre-heat the target fuel in direct-drive inertial confinement fusion (ICF) experiments, potentially impeding the assembly of sufficient fuel areal density for ignition.¹⁻⁴ TPD is a three-wave parametric instability in which an incident photon at frequency ω_0 decays into two electron-plasma waves (plasmons) with frequencies near $\omega_0/2$. Because of the resonant nature of this process, it is restricted to a small range of electron densities near the quarter-critical density. The instability threshold intensity is known to decrease and the saturation levels increase as the plasma density scale length increases.⁵⁻⁸

The basic theory of TPD was developed long ago^{5,6} along with a number of numerical simulations;⁷⁻¹³ however, experimental verification has been of a qualitative nature at best. Quantitative predictions for the suprathermal-electron generation are only now starting to emerge from simulations but have not yet been compared with experimental data.¹³ Even though some experiments used multiple overlapping beams,¹ their analysis has always been made in the single-beam approximation. This was based on the belief that the single-beam intensity dominates the scaling of the TPD instability even in experiments with multiple overlapping beams.

This article presents for the first time clear evidence for strong overlapping-beam effects on suprathermal-electron generation in both spherical and planar experiments. TPD instability was found to scale predominantly with overlapped intensity, which is defined as the incoherent sum of the interaction-beam intensities. The single-beam intensity and the number of overlapped beams did not significantly affect the observed scaling. There are several characteristic signatures for TPD instability: $3\omega_0/2$ and $\omega_0/2$ emission in the scattered light,^{4,14} a hard component (>20 keV) in the continuum x-ray bremsstrahlung spectrum,¹⁵ an energetic tail in the suprathermal electron spectrum,¹⁶ and K_α emission from cold material due to preheat.^{17,18} On the OMEGA laser system¹⁹ TPD instability is monitored using a $3\omega_0/2$ spectrometer and a time-resolved, scintillator-based, four-channel hard-x-ray detector

system.²⁰ The observed hard x rays can be attributed only to TPD instability since competing production mechanisms such as stimulated Raman scattering (SRS) are not seen in significant amounts in these experiments.^{21,22} In addition, the electron temperatures inferred from the hard-x-ray signals are well above those measured for SRS,²³ and the $3\omega_0/2$ signature is seen in all of the reported experiments.

The experiments in spherical geometry used targets of varying diameters similar to those described in Ref. 24. Gas-filled CH targets (900- to 1100- μm diameter, ~ 27 - μm wall thickness, and 20 atm of D_2 fill) were irradiated with 60 beams at 351-nm wavelength, with 1-ns square pulses and ~ 23 -kJ total energy. All beams were smoothed by two-dimensional smoothing by spectral dispersion²⁵ with 1-THz bandwidth in the UV and polarization smoothing.²⁶ Standard OMEGA phase plates²⁷ were used throughout with a spot size of ~ 0.5 -mm FWHM and a speckle-averaged peak intensity of $\sim 2 \times 10^{14}$ W/cm². The total overlapped intensity on target varied between 6.0×10^{14} W/cm² and 8.5×10^{14} W/cm², due to the varying target surface area, while the peak single-beam intensity on target was virtually unchanged. One-dimensional *LILAC*²⁸ hydrodynamic simulations show a rapidly growing radial density scale length at a quarter-critical density that reaches ~ 100 μm midway through the pulse. This is followed by a slower growth to ~ 150 μm at the end of the pulse. The coronal electron temperature is predicted to be relatively constant, with a typical value of ~ 2.5 keV. Figure 94.13 shows the hard-x-ray and $3\omega_0/2$ signatures of the TPD instability from the spherical experiments as a function of overlapped intensity. The suprathermal-electron temperature as inferred from the hard-x-ray spectrum²⁰ changes very little, which is consistent with earlier observations.^{2,3} In contrast, the measured hard-x-ray energy scales exponentially with overlapped intensity as $\exp(I_{14}/1.2)$, where I_{14} is the intensity in units of 10^{14} W/cm². This behavior strongly suggests that the TPD instability in the OMEGA implosion experiments scales primarily with the overlapped intensity rather than the single-beam intensity. Even though the overlapped intensity varies by only 30%, the hard-x-ray signature from the suprathermal elec-



E11103a

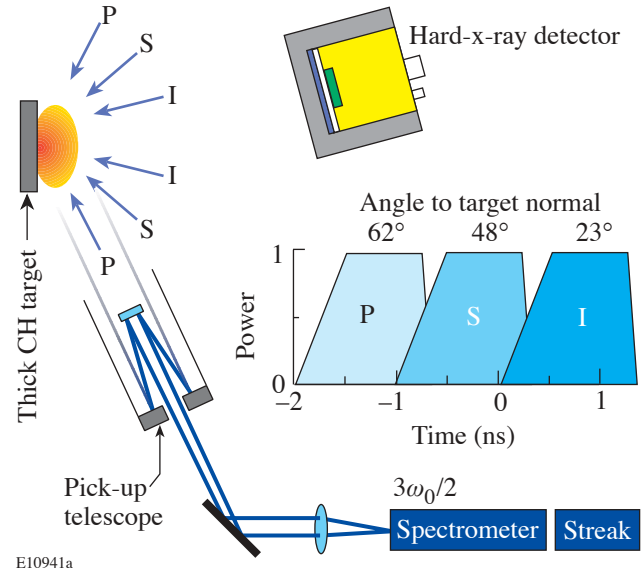
Figure 94.13

Signatures from TPD instability observed in a spherical implosion experiment on OMEGA using targets of varying diameter. The hard-x-ray (>50-keV) signal, the $3\omega_0/2$ emission, and the suprathermal-electron temperature inferred from the hard-x-ray spectrum scale with the total overlapped intensity. The peak single-beam intensity is kept constant.

trons changed by a factor of 10 and the $3\omega_0/2$ signature varied by a factor of 5.

Future direct-drive ignition experiments on the National Ignition Facility (NIF)²⁹ are expected to generate longer scale lengths ($\sim 500 \mu\text{m}$) at a higher overlapped laser intensity ($1.3 \times 10^{15} \text{ W/cm}^2$). Since these conditions are potentially more vulnerable to suprathermal-electron generation, a set of dedicated planar experiments was carried out at longer scale lengths closer to those expected on the NIF. The experimental layout (Fig. 94.14) was similar to that of Ref. 30. CH targets of $100\text{-}\mu\text{m}$ thickness and 5-mm diameter were sequentially irradiated with nine primary (P) beams, followed by six secondary (S) beams and two to six interaction (I) beams. The interaction beams were incident at $\sim 23^\circ$ to the target normal, and the P and S beams were at $\sim 62^\circ$ and $\sim 48^\circ$, respectively. The beam-smoothing conditions were identical to the spherical experiments. The P and S beams had standard phase plates that were defocused ($\sim 1\text{-mm}$ FWHM) with speckle-averaged peak intensities of $\sim 5 \times 10^{13} \text{ W/cm}^2$. The six interaction beams used either standard phase plates at nominal focus ($\sim 2 \times 10^{14} \text{ W/cm}^2$) or high-intensity phase plates ($\sim 0.25\text{-mm}$ FWHM) at $8 \times 10^{14} \text{ W/cm}^2$. The individual beam energies were varied between 180 and 360 J, and the laser pulse shape was well approximated by a 500-ps ramp followed by a 1-ns flat portion. Two-dimensional hydrodynamic *SAGE*³¹ simulations, which

generally replicate these experimental configurations very well,²¹ predict typical electron temperatures of $\sim 2.5 \text{ keV}$ and a relatively constant electron-density scale length of $\sim 350 \mu\text{m}$ for six overlapped interaction beams with standard phase plates. For six high-intensity interaction beams, the predicted electron temperatures rise to $\sim 4.5 \text{ keV}$ with density scale lengths reduced to $\sim 180 \mu\text{m}$. Simulations for fewer than six overlapped beams generally show similar scale lengths at lower temperatures.

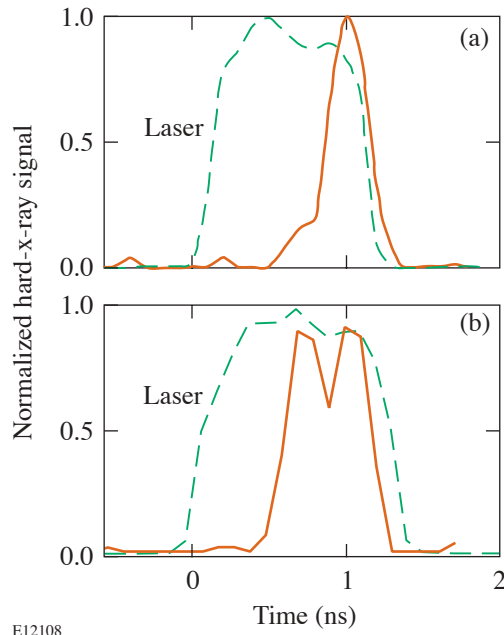


E10941a

Figure 94.14

Schematic layout of planar experiments using three sets of laser beams: nine primary (P) beams, six secondary (S) beams, and two to six interaction (I) beams. The pulse sequence, pulse shape, and approximate angles of incidence are indicated. The TPD instability is monitored using a streaked optical $3\omega_0/2$ spectrometer and a time-resolved, scintillator-based, four-channel hard-x-ray detector system (only one channel is shown).

Figure 94.15 shows the time-resolved hard-x-ray signal (>50 keV) from a spherical implosion (a) and a planar experiment using six overlapped beams with standard phase plates (b), with the same overlapped intensity of $\sim 10^{15} \text{ W/cm}^2$. In both cases the signal is significantly delayed with respect to the laser pulse and vanishes rapidly at the end of the laser pulse. This delay is not fully understood, but the difference between the spherical and planar experiments is probably due to the pre-existing scale length at the start of the interaction beam for the planar case. The highly nonlinear scaling of the TPD instability with intensity can be observed in the strong amplification of the laser-intensity variations.



E12108

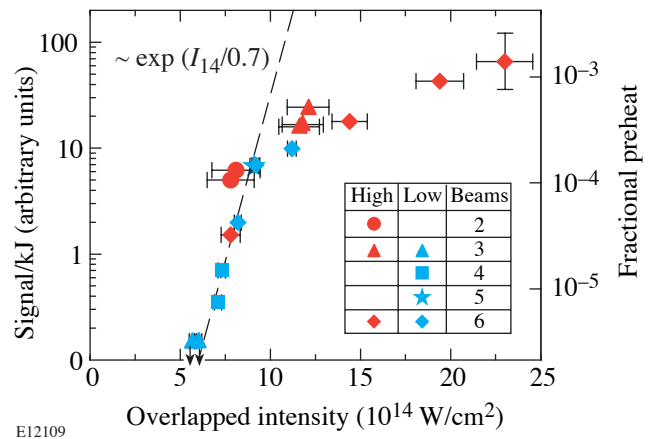
Figure 94.15

Time-resolved hard-x-ray (>50 -keV) emission (solid line) from a spherical implosion experiment (a) and a planar long-scale-length experiment using six beams with standard phase plates (b). The time history of the laser pulse (dashed line) is shown for comparison. The overlapped laser intensity was $\sim 10^{15}$ W/cm 2 in both cases.

Figure 94.16 shows time-integrated hard-x-ray signals for $E_x > 50$ keV (normalized to the total interaction-beam energy for the planar experiments with both standard and high-intensity phase plates). The pointing accuracy (~ 50 - μ m rms) of the overlapping beams is the dominant contribution to the error for the overlapped intensity. The measurement error of the hard-x-ray signal is $<10\%$, about the size of the symbols used. Even though the plasma conditions vary considerably in both scale length and temperature, the hard-x-ray signal is primarily a function of overlapped interaction-beam intensity. The number of overlapped beams and the single-beam intensity seem to be of almost no importance. Remarkably all data can be fit to a universal exponential scaling $\sim \exp(I_{14}/0.7)$ below an intensity of 10^{15} W/cm 2 , even stronger than that observed in spherical geometry. Above 10^{15} W/cm 2 the scaling of the hard-x-ray signal with intensity changes significantly and is much weaker. The fact that the overlapped intensity governs the scaling of TPD is most easily seen by comparing the signals from six overlapped beams with standard phase plates at an intensity of 11.2×10^{14} W/cm 2 to those of three beams with standard phase plates at an intensity of 5.7×10^{14} W/cm 2 . If single-beam intensity were to govern suprathermal-electron

generation, three beams would produce the same hard-x-ray signal per kJ of laser energy as six beams, but actual experiments show $>60\times$ reduction, which means that the hard-x-ray signals are actually below the detector threshold.

An absolute measurement of the hard x rays is necessary to infer the heating of the targets from suprathermal electrons. Because the absolute calibration of the hard-x-ray detectors is not very accurate,²⁰ the detectors have been cross-calibrated with preheat measurements using K_α spectroscopy^{32,33} on CH targets with embedded high-Z layers. These layers consisted of 5 μ m of titanium followed by 40 μ m of vanadium, covered with 20 μ m of CH on all sides to avoid direct laser interaction. Consequently the generation of suprathermal electrons is the same as in the primary experiments. The titanium layer absorbs the coronal x radiation without significantly affecting the suprathermal electrons, which then excite K_α radiation in the vanadium layer. The total energy in the vanadium K_α line observed on the back of the target is a good measure of the energy deposited by the electrons and thus the preheat.³² Thus calibrated, the signals from the hard-x-ray detectors can be used to infer the level of preheat of the CH planar targets. The inferred fractional preheat (preheat energy



E12109

Figure 94.16

Time-integrated hard-x-ray signals ($E_x > 50$ keV) as a function of overlapped interaction-beam intensity for planar experiments. Two to six beams are used with both standard and high-intensity phase plates at beam energies between 180 and 360 J. The error for the intensity is determined by the beam-pointing accuracy of ~ 50 - μ m rms of the overlapping beams. The relative error of the hard-x-ray signal is about the size of the symbols used ($<10\%$). An exponential scaling $\sim \exp(I_{14}/0.7)$ below an overlapped intensity of 10^{15} W/cm 2 (dashed line) is shown for comparison. The axis on the right corresponds to the estimate of the target preheat based on the calibration using K_α spectroscopy. The uncertainty of the calibration ($\sim 50\%$) is indicated with the error bar on the far-right data point.

normalized to incident laser energy) is shown on the right axis of Fig. 94.16. The uncertainty of these numbers is determined by the accuracy of the K_α cross-calibration of $\sim 50\%$. It is encouraging that the preheat level lies below 0.1% for intensities around 1.3×10^{15} W/cm², the peak intensity required for NIF direct-drive experiments.

In conclusion, experimental evidence from both spherical and long-scale-length planar experiments shows clearly that the total overlapped intensity governs the scaling of the suprathermal-electron production while the single-beam intensity is of lesser importance. Presently no theoretical explanation of this behavior exists, but simulations of the nonlinear saturated stage of the TPD instability¹² suggest that the spectrum of the plasma waves broadens considerably, which makes it conceivable that overlapping beams might act on the same plasmon. The exponential scaling seen in both experiments at overlapped intensities below 10^{15} W/cm² is even stronger in the planar case than that observed in the spherical experiments. This may be due to the presence of a long (>100 μm) and slowly evolving density scale length right from the start of the interaction beam in the planar experiments, which is correlated with an earlier onset of hard-x-ray emission, as compared to the spherical experiments. The origin of the consistently observed change in scaling with intensity of the fractional-preheat levels above 10^{15} W/cm² for all studied plasma density scale lengths and temperatures remains unclear at this time. There could potentially be a correlation with the filamentation instability, which has a similar threshold.³⁴ Nevertheless, this observation increases the confidence that the preheat levels from suprathermal electrons are manageable for direct-drive ignition experiments on the NIF.

ACKNOWLEDGMENT

This work was supported by the U.S. Department of Energy Office of Inertial Confinement Fusion under Cooperative Agreement No. DE-FC03-92SF19460, the University of Rochester, and the New York State Energy Research and Development Authority. The support of DOE does not constitute an endorsement by DOE of the views expressed in this article.

REFERENCES

1. D. W. Phillion *et al.*, Phys. Rev. Lett. **49**, 1405 (1982).
2. D. M. Villeneuve, R. L. Keck, B. B. Afeyan, W. Seka, and E. A. Williams, Phys. Fluids **27**, 721 (1984).
3. C. Rousseaux *et al.*, Phys. Fluids B **4**, 2589 (1992).

4. W. Seka, R. E. Bahr, R. W. Short, A. Simon, R. S. Craxton, D. S. Montgomery, and A. E. Rubenchik, Phys. Fluids B **4**, 2232 (1992).
5. C. S. Liu and M. N. Rosenbluth, Phys. Fluids **19**, 967 (1976).
6. A. Simon, R. W. Short, E. A. Williams, and T. Dewandre, Phys. Fluids **26**, 3107 (1983).
7. A. B. Langdon, B. F. Lasinski, and W. L. Kruer, Phys. Rev. Lett. **43**, 133 (1979).
8. B. F. Lasinski and A. B. Langdon, Lawrence Livermore National Laboratory, Livermore, CA, UCRL-50021-77, 4-49 (1978).
9. L. V. Powers and R. L. Berger, Phys. Fluids **27**, 242 (1984).
10. *Ibid.*, **28**, 2419 (1985).
11. R. L. Berger and L. V. Powers, *ibid.*, 2895 (1985).
12. D. F. DuBois, D. A. Russell, and H. A. Rose, Phys. Rev. Lett. **74**, 3983 (1995).
13. D. A. Russell and D. F. DuBois, Phys. Rev. Lett. **86**, 428 (2001).
14. J. Meyer and Y. Zhu, Phys. Rev. Lett. **71**, 2915 (1993).
15. R. L. Keck, L. M. Goldman, M. C. Richardson, W. Seka, and K. Tanaka, Phys. Fluids **27**, 2762 (1984).
16. N. A. Ebrahim *et al.*, Phys. Rev. Lett. **45**, 1179 (1980).
17. B. Yaakobi, I. Pelah, and J. Hoose, Phys. Rev. Lett. **37**, 836 (1976).
18. J. D. Hares *et al.*, Phys. Rev. Lett. **42**, 1216 (1979).
19. T. R. Boehly, D. L. Brown, R. S. Craxton, R. L. Keck, J. P. Knauer, J. H. Kelly, T. J. Kessler, S. A. Kumpan, S. J. Loucks, S. A. Letzring, F. J. Marshall, R. L. McCrory, S. F. B. Morse, W. Seka, J. M. Soures, and C. P. Verdon, Opt. Commun. **133**, 495 (1997).
20. C. Stoeckl, V. Yu. Glebov, D. D. Meyerhofer, W. Seka, B. Yaakobi, R. P. J. Town, and J. D. Zuegel, Rev. Sci. Instrum. **72**, 1197 (2001).
21. S. P. Regan, D. K. Bradley, A. V. Chirokikh, R. S. Craxton, D. D. Meyerhofer, W. Seka, R. W. Short, A. Simon, R. P. J. Town, B. Yaakobi, J. J. Carroll III, and R. P. Drake, Phys. Plasmas **6**, 2072 (1999).
22. R. L. McCrory, R. E. Bahr, T. R. Boehly, T. J. B. Collins, R. S. Craxton, J. A. Delettrez, W. R. Donaldson, R. Epstein, V. N. Goncharov, R. Q. Gram, D. R. Harding, P. A. Jaanimagi, R. L. Keck, J. P. Knauer, S. J. Loucks, F. J. Marshall, P. W. McKenty, D. D. Meyerhofer, S. F. B. Morse, O. V. Gotchev, P. B. Radha, S. P. Regan, W. Seka, S. Skupsky, V. A. Smalyuk, J. M. Soures, C. Stoeckl, R. P. J. Town, M. D. Wittman, B. Yaakobi, J. D. Zuegel, R. D. Petrasso, D. G. Hicks, and C. K. Li, in *Inertial Fusion Sciences and Applications 99*, edited by C. Labaune, W. J. Hogan, and K. A. Tanaka (Elsevier, Paris, 2000), pp. 43–53.
23. R. P. Drake *et al.*, Phys. Rev. A **40**, 3219 (1989).

24. D. D. Meyerhofer, J. A. Delettrez, R. Epstein, V. Yu. Glebov, V. N. Goncharov, R. L. Keck, R. L. McCrory, P. W. McKenty, F. J. Marshall, P. B. Radha, S. P. Regan, S. Roberts, W. Seka, S. Skupsky, V. A. Smalyuk, C. Sorce, C. Stoeckl, J. M. Soures, R. P. J. Town, B. Yaakobi, J. D. Zuegel, J. Frenje, C. K. Li, R. D. Petrasso, D. G. Hicks, F. H. Séguin, K. Fletcher, S. Padalino, M. R. Freeman, N. Izumi, R. Lerche, T. W. Phillips, and T. C. Sangster, *Phys. Plasmas* **8**, 2251 (2001).
25. S. Skupsky, R. W. Short, T. Kessler, R. S. Craxton, S. Letzring, and J. M. Soures, *J. Appl. Phys.* **66**, 3456 (1989).
26. T. R. Boehly, V. A. Smalyuk, D. D. Meyerhofer, J. P. Knauer, D. K. Bradley, R. S. Craxton, M. J. Guardalben, S. Skupsky, and T. J. Kessler, *J. Appl. Phys.* **85**, 3444 (1999).
27. T. J. Kessler, Y. Lin, J. J. Armstrong, and B. Velazquez, in *Laser Coherence Control: Technology and Applications*, edited by H. T. Powell and T. J. Kessler (SPIE, Bellingham, WA, 1993), Vol. 1870, pp. 95–104.
28. M. C. Richardson, P. W. McKenty, F. J. Marshall, C. P. Verdon, J. M. Soures, R. L. McCrory, O. Barnouin, R. S. Craxton, J. Delettrez, R. L. Hutchison, P. A. Jaanimagi, R. Keck, T. Kessler, H. Kim, S. A. Letzring, D. M. Roback, W. Seka, S. Skupsky, B. Yaakobi, S. M. Lane, and S. Prussin, in *Laser Interaction and Related Plasma Phenomena*, edited by H. Hora and G. H. Miley (Plenum Publishing, New York, 1986), Vol. 7, pp. 421–448.
29. P. W. McKenty, V. N. Goncharov, R. P. J. Town, S. Skupsky, R. Betti, and R. L. McCrory, *Phys. Plasmas* **8**, 2315 (2001).
30. W. Seka, H. A. Baldis, J. Fuchs, S. P. Regan, D. D. Meyerhofer, C. Stoeckl, B. Yaakobi, R. S. Craxton, and R. W. Short, *Phys. Rev. Lett.* **89**, 175002 (2002).
31. R. S. Craxton and R. L. McCrory, *J. Appl. Phys.* **56**, 108 (1984).
32. B. Yaakobi, C. Stoeckl, T. Boehly, D. D. Meyerhofer, and W. Seka, *Phys. Plasmas* **7**, 3714 (2000).
33. B. Yaakobi, C. Stoeckl, T. R. Boehly, R. S. Craxton, D. D. Meyerhofer, and W. D. Seka, in *26th European Conference on Laser Interaction with Matter*, edited by M. Kalal, K. Rohlena, and M. Siñor (SPIE, Bellingham, WA, 2001), Vol. 4424, pp. 392–401.
34. Laboratory for Laser Energetics LLE Review **91**, 93, NTIS document No. DOE/SF/19460-458 (2002). Copies may be obtained from the National Technical Information Service, Springfield, VA 22161.